A DOUBLE CLUSTER AT THE CORE OF 30 DORADUS[*]

E. Sabbi[1], D. J. Lennon[2], M. Gieles[3], S. E. de Mink[1,4,6], N. R. Walborn[1], J. Anderson[1], A. Bellini[1],
N. Panagia[1], R. van der Marel[1], and J. Maíz Apellániz[5]

[1] Space Telescope Science Institute, 3700 San Martin Drive, Baltimore, MD 21218, USA; sabbi@stsci.edu
[2] ESA/STScI, 3700 San Martin Drive, Baltimore, MD 21218, USA
[3] Institute of Astronomy, University of Cambridge, Madingley Road, Cambridge CB3 0HA, UK
[4] Johns Hopkins University, 3400 N. Charles St., Baltimore, MD 21218, USA
[5] Instituto de Astrofísica de Andalucía-CSIC, Glorieta de la Astronomía s/n, E-18008, Granada, Spain
Received 2012 June 20; accepted 2012 July 2; published 2012 July 17

ABSTRACT

Based on an analysis of data obtained with the Wide Field Camera 3 on the *Hubble Space Telescope* we report the identification of two distinct stellar populations in the core of the giant H II region 30 Doradus in the Large Magellanic Cloud. The most compact and richest component coincides with the center of R136 and is ∼1 Myr younger than a second more diffuse clump, located ∼5.4 pc toward the northeast. We note that published spectral types of massive stars in these two clumps lend support to the proposed age difference. The morphology and age difference between the two sub-clusters suggests that an ongoing merger may be occurring within the core of 30 Doradus. This finding is consistent with the predictions of models of hierarchical fragmentation of turbulent giant molecular clouds, according to which star clusters would be the final products of merging smaller sub-structures.

Key words: galaxies: star clusters: individual (30 Doradus) – galaxies: star formation – Magellanic Clouds

Online-only material: color figures

1. INTRODUCTION

As the most luminous and best known massive star-forming region in the Local Group (Kennicutt 1984), the Tarantula Nebula in the Large Magellanic Cloud (LMC) offers us the unique opportunity to investigate the process of star formation (SF) in an environment that, in many ways (such as metallicity, dust content, and SF rate), resembles the extreme conditions of the early universe and distant star-forming regions. The SF history of Tarantula's ionizing cluster NGC 2070 (a.k.a. 30 Dor) is complex. Walborn & Blades (1997) defined 30 Dor as a two-stage starburst, in which the radiation from the compact core R136 has triggered a new generation of stars at a projected distance of ∼1′ (corresponding to ∼15 pc at the distance of the LMC).

The complexity of NGC 2070 is also reflected in its atypical luminosity profile, which shows a break at ∼10″ (∼2.5 pc) and a bump at ∼30″ (∼7 pc; Mackey & Gilmore 2003). More recent observations in the near IR with multiconjugate adaptive optics indicate that the innermost ∼30″ of the luminosity profile can be fitted with a single Elson et al. (1987; EFF) power law, once the asymmetric shape of 30 Dor is taken into account (Campbell et al. 2010).

Here, we take advantage of the high spatial resolution and sensitivity of the Wide Field Camera 3 (WFC3) on board of the *Hubble Space Telescope* (*HST*) to study the innermost ∼2′44″ × 2′44″ of NGC 2070. In particular, we use public UVIS and IR channel observations (P.I. R.W. O'Connell, GO-11360) to characterize the spatial distribution of its stellar populations.

2. DATA

Deep WFC3 observations of R136, the core of NGC 2070, were retrieved from the Mikulski Archive for Space Telescopes (MAST). The data set consists of six broadband filters (F336W, F438W, F555W, F814W, F110W, and F160W), ranging from the near-UV to the near-IR, and is described in detail in De Marchi et al. (2011). The images were processed through the standard calibration pipeline CALWF3, using the most up-to-date calibration files.

Positions and fluxes of the stars in the WFC3/UVIS images were measured using img2xym_wfc3uv, while we used img2xym_wfc3ir to measure positions and fluxes in the WFC3/IR images. Both codes were adapted from img2xym_WFI (Anderson et al. 2006). The astrometry and photometry of WFC3/UVIS data were corrected for pixel area variations and geometric distortion as in Bellini & Bedin (2009) and Bellini et al. (2011), while for the WFC3/IR data we used the solutions from J. Anderson et al. (2012, in preparation). Stars were detected independently in each filter. The WFC3 photometric catalogs were calibrated into the Vegamag photometric system using the most up-to-date values of the zero points, available at the WFC3 Web site,[7] and then combined into a single catalog. Approximately 3000 stars with photometric errors smaller than <0.15 mag were found in all six bands.

3. ANALYSIS

Figure 1 shows three color–magnitude diagrams (CMDs) of the stars found in the region covered by the UVIS observations for different combinations of the filters F336W, F438W, F555W, and F814W. In each plot, stars were selected to have photometric errors <0.15 in both the plotted filters. Padova isochrones (dashed lines; Marigo et al. 2008) for main sequence (MS) and evolved stars, and Pisa isochrones (continuous lines;

---

7 http://www.stsci.edu/hst/wfc3/phot_zp_lbn
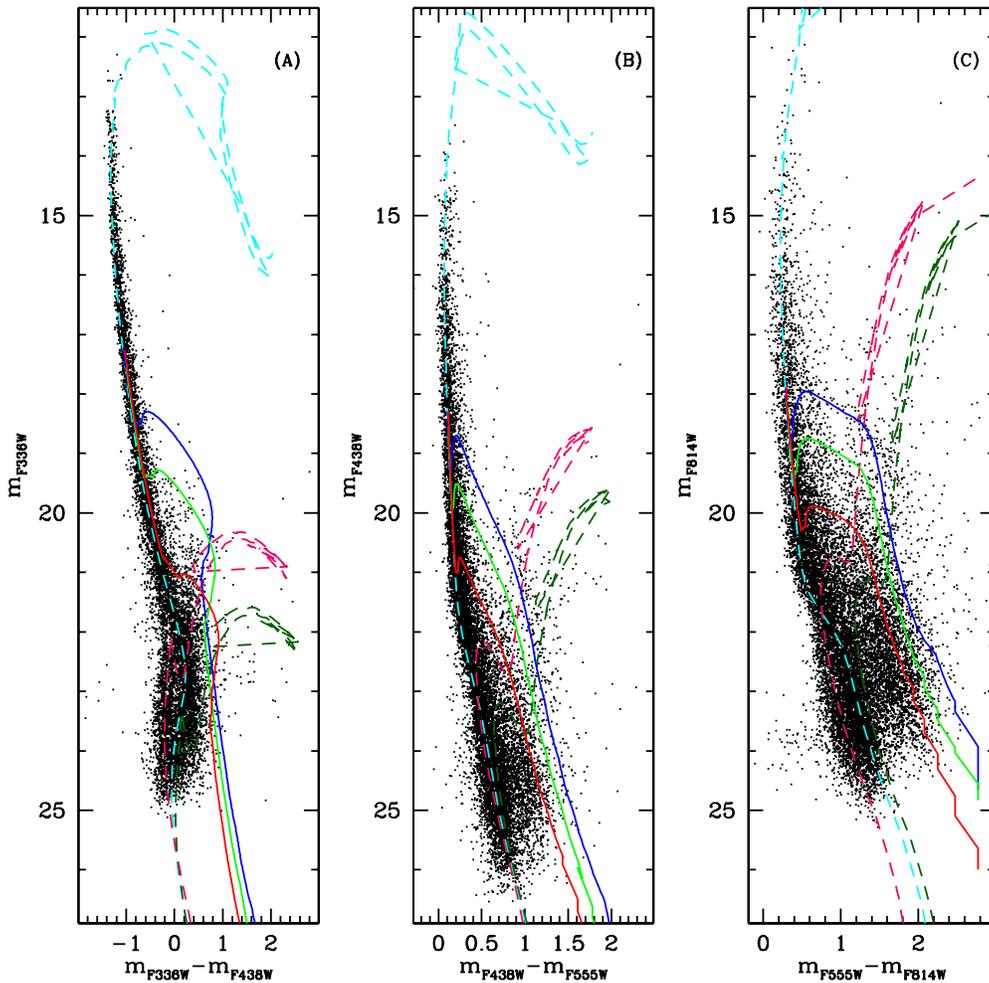
Figure 1. CMDs of m_{F336W} vs. $m_{F336W} - m_{F438W}$ (A), m_{F438W} vs. $m_{F438W} - m_{F555W}$ (B), and m_{F814W} vs. $m_{F555W} - m_{F814W}$ (C), of the stars found in the NGC 2070 region with photometric errors <0.15 mag in both filters. Pisa isochrones (solid; Tognelli et al. 2011) for PMS stars of metallicity $Z = 0.008$ and ages = 1, 2, and 5 Myr are shown in blue, green, and red, respectively. The dashed isochrones are from Marigo et al. (2008). A 10 Myr old stellar population with $Z = 0.008$ is shown in cyan. A 4 Gyr old stellar population with $Z = 0.004$ and two distinct values of reddening ($E(B - V) = 0.14$ and 0.4) is shown in magenta and dark green, respectively.

(A color version of this figure is available in the online journal.)

Tognelli et al. 2011) for pre-main sequence (PMS) stars, are superimposed to guide the eye. In doing this we assumed a distance of 50 kpc (Schaefer et al. 2008) and a metallicity $Z = 0.008$ (Helling et al. 2000). Isochrones are also corrected for reddening.

Inspection of these CMDs shows that the stellar content is complex: the bright and blue upper MS (i.e., $m_{F814} \lesssim 21$; $m_{F555W} - m_{F814} \lesssim 0.6$ in panel (C)) is composed of intermediate- and high-mass stars, but at redder colors (i.e., $m_{F555W} - m_{F814W} \gtrsim 1.5$ in panel (C)) the majority of the sources are PMS stars in the mass range $0.5 \lesssim M \lesssim 5.0 \, M_\odot$ and ages $\gtrsim 1$ Myr. Pisa isochrones show that PMS stars become fainter and bluer with age, to the point that after ~10 Myr they are indistinguishable from the low-mass MS ($m_{F814W} \gtrsim 21$; $m_{F555W} - m_{F814} \lesssim 1.0$ in panel (C)).

Figure 2 shows the stellar density distributions in the $\sim 2'44'' \times 2'44''$ area around R136 in the filters F336W, F438W, F555W, F184W, and F160W. In each map the pixel scale is $2''$, and the density levels are the square root of the number of stars. The spatial distribution of the stars in the F336W, F438W, and F555W maps is remarkably similar, with the majority of the stars "clustered" at R.A. $= 05^h38^m42\overset{s}{.}6$, decl. $= -69°06'03''$, J2000, which coincides with the center of 30 Dor

(Figures 3 and 4). The apparent decrease of star counts in the F814W and F160W maps where R136 is located is caused by the high crowding, since no completeness corrections were applied to the maps.

In each map the density contours are not spherical. On the contrary, they show an arc that departs from R136 to the northeast. This feature is clearly visible in all the filters, from the UV to the near IR, making it unlikely that local high reddening can be at the origin of this structure. The low impact of variable reddening in the stellar counts is also shown by the ratio between the F160W and F555W isodensity maps (Figure 2, lower-right panel).

In Figure 5, the (m_{F555W}, $m_{F555W} - m_{F814W}$) CMD of the stars found within $10''$ from the center of R136 is compared to that of the stars found in a $14''.4 \times 27''.4$ box centered on the northeast clump (see also Figure 4). In both plots, most of the brighter stars ($m_{F555W} \lesssim 19.5$) trace a well-defined blue ($m_{F555W} - m_{F814W} \lesssim 0.5$) upper MS, while below this value the majority of the stars show the red colors typical of intermediate- and low-mass ($0.5 \lesssim M \lesssim 5.3 \, M_\odot$) PMS stars. Although the northeast clump is less then $\sim 22''$ (corresponding to a projected distance of ~5.4 pc) away from R136, the redder and broader upper MS of R136 indicates that the two populations are affected
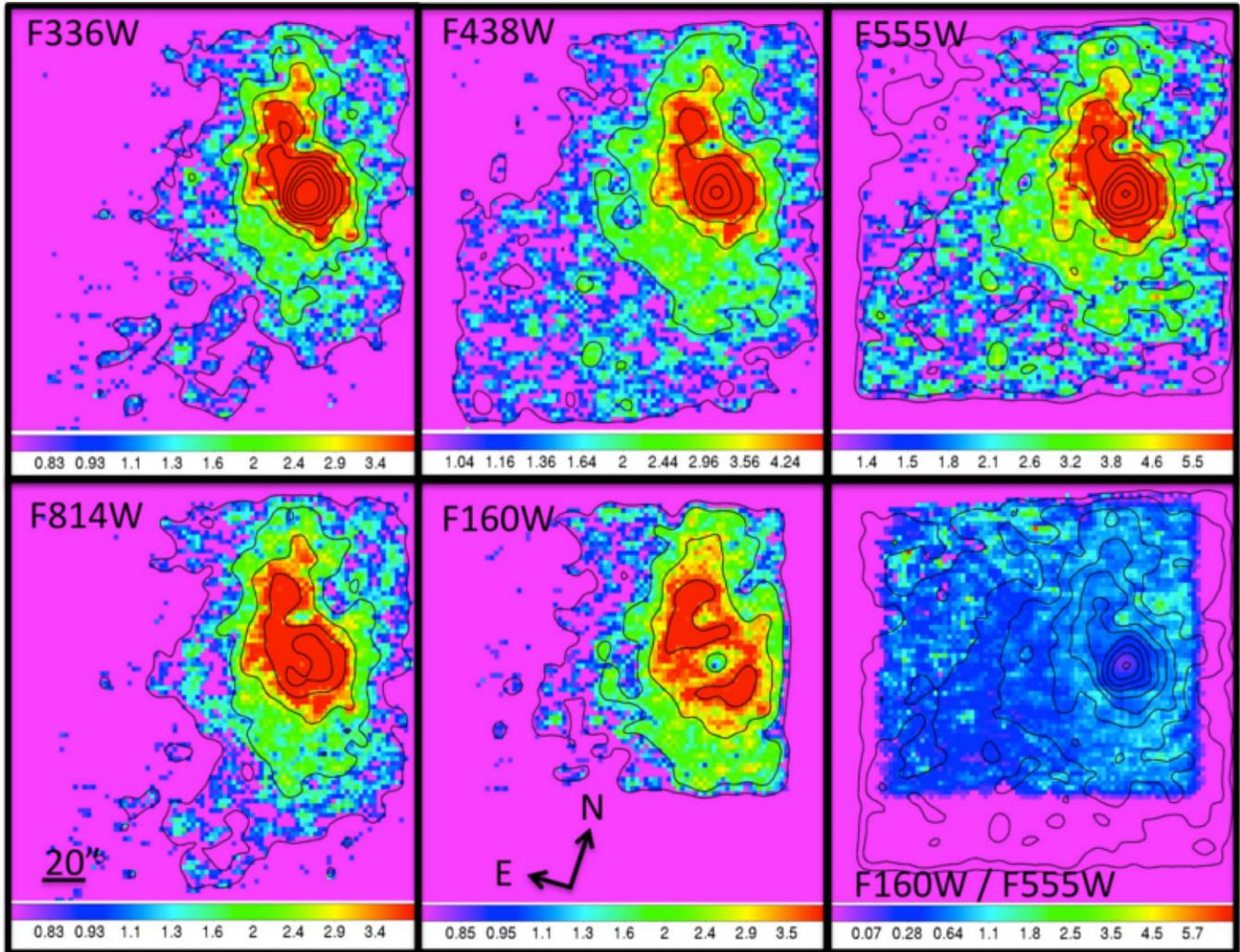
Figure 2. Stellar density charts of the stars found in the core of NGC 2070 in the filters F336W, F438W, F555W, F814W, and F160W. In each map, the highest level is five times higher than the lower one. The lower-right plot shows the ratio between the F160W and F555W maps. Isodensity contours from the F555W map are plotted for reference. In all the maps north is up, and east is to the left.

(A color version of this figure is available in the online journal.)

by different dust extinction. Isochrone fitting of the upper MS indicate that $A_{F555W} = 1.207$ is sufficient for the northeast clump, but for R136 $A_{F555W} = 1.525$ is more appropriate. The same values have been obtained by applying a procedure similar to that used in De Marchi et al. (2011)

It is commonly known that the steepness of the upper MS and the paucity of massive stars makes it challenging to identify the MS turnoff, and even harder to distinguish age differences of the order of few Myr, in star clusters younger than $\lesssim 5$ Myr using isochrone-fitting only. In such clusters, a more robust age indicator is the luminosity of the turn-on, defined as the locus of the CMD where the PMS stars join the MS (Stauffer 1980; Belikov et al. 1998; Baume et al. 2003; Cignoni et al. 2010). The age of a cluster can be defined as the time spent in the PMS phase by its most massive PMS star.

The comparison between the CMDs of the two components shows that PMS stars in R136 are more than ∼0.5 mag brighter compared to those found in the northeast clump. Since R136 is affected by a higher reddening than the northeast clump, we conclude that PMS stars in R136 are intrinsically brighter, and therefore that in R136 SF lasted for at least 1 Myr more than in

the northeast clump.[8] It is possible to see the northeast clump also in Figure 11 of De Marchi et al. (2011), where the spatial distribution of PMS stars younger than 4 Myr is compared to that of older objects with active mass accretion.

4. DISCUSSION AND CONCLUSIONS

We used deep *HST*/WFC3 UV, optical and near-IR observations of the core of 30 Dor to study its stellar content. In all the filters, we identified a dual structure that cannot be attributed to dust extinction. A careful analysis of the stellar content of the clumps indicates that, while the northeast clump formed the majority of its stars between 2 and 5 Myr ago, R136 started to form stars likely ∼2 Myr ago and was still active ∼1 Myr ago.

In retrospect, there are substantial indications in the literature that the northeast clump comprises a distinct, more evolved entity. Its two brightest members, R141 and R142, are early B supergiants that must be older than the denizens of R136

---

[8] We can exclude that the difference in magnitude between the two clumps is due to the distance, because $\Delta m_{F555W} \simeq 1$ would imply that the northeast clump would be at ∼79.5 kpc, far beyond even the Small Magellanic Cloud.
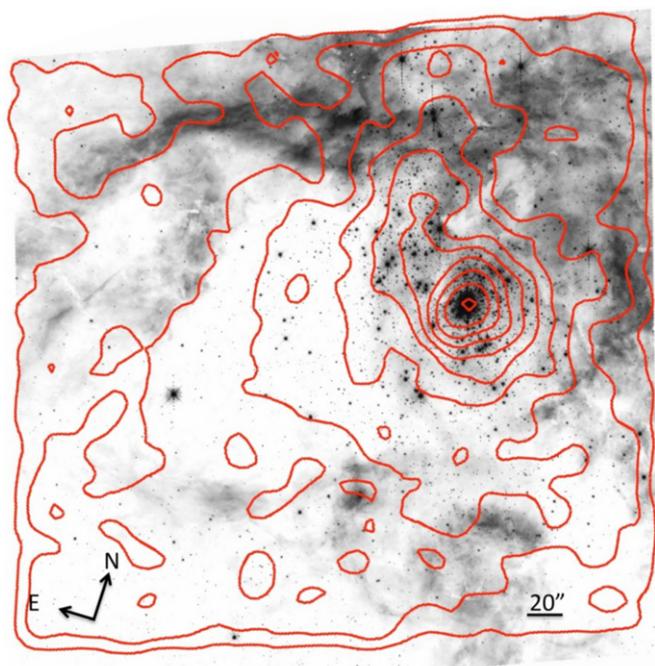
Figure 3. UVIS image of 30 Dor in the F555W filter. North is up, east to the left. Isodensity contours as derived in Figure 2 are shown for reference.

(A color version of this figure is available in the online journal.)

itself (Feast et al. 1960; Parker 1993). Many of the fainter late-O/early-B stars are also evolved and subject to the same age argument (Walborn & Blades 1997; Massey & Hunter 1998; Bosch et al. 1999). In an analysis of SF in the 30 Dor core based upon these observations, Selman (1999) proposed three sequential events with mean ages less than 1.5 Myr, 2.5 Myr, and 5 Myr; their Figure 9 shows that the first is strongly concentrated toward R136, while the heaviest concentration of the intermediate and old objects coincides with the northeast clump.

The age difference between R136 and the northeast clump can also explain the, until now, puzzling presence of two WC stars in 30 Dor, as these highly evolved objects are seldom found in giant H ɪɪ regions. One of them, Mk 33d, is located in an apparent multiple system at the inner edge of the northeast clump (Melnick 1985), while the northward tail on the northeast clump encompasses the multiple system R140 containing the other WC along with two WN's (Moffat et al. 1987). Finally, even the isolated M supergiant IR18 (McGregor & Hyland 1981) somewhat farther to the northeast, long considered a field interloper, could actually be associated with the older clump. Positions of the mentioned stars with respect to the two sub-clusters are shown in Figure 4.

This is, of course, a complex three-dimensional region, and some earlier spectral types also appear in the predominantly older fields, particularly in the Mk 33 system. The O2 If*/WN5 object Mk 30 (Crowther & Walborn 2011) that lies adjacent to
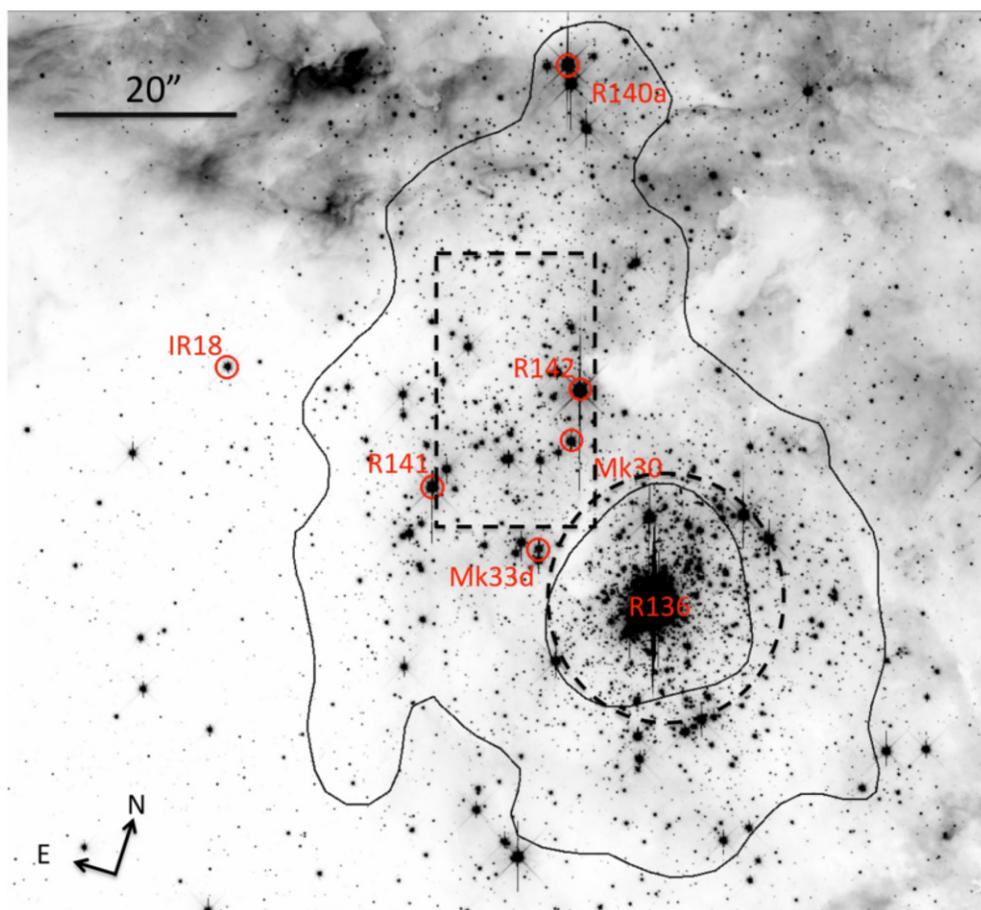
Figure 4. F555W UVIS image zoomed on the center of 30 Dor. The dashed circle and rectangle indicate the regions used to derive the CMDs shown in Figure 5. Stars mentioned in the discussion are highlighted. Two isodensity contours are shown to guide the eye.

(A color version of this figure is available in the online journal.)
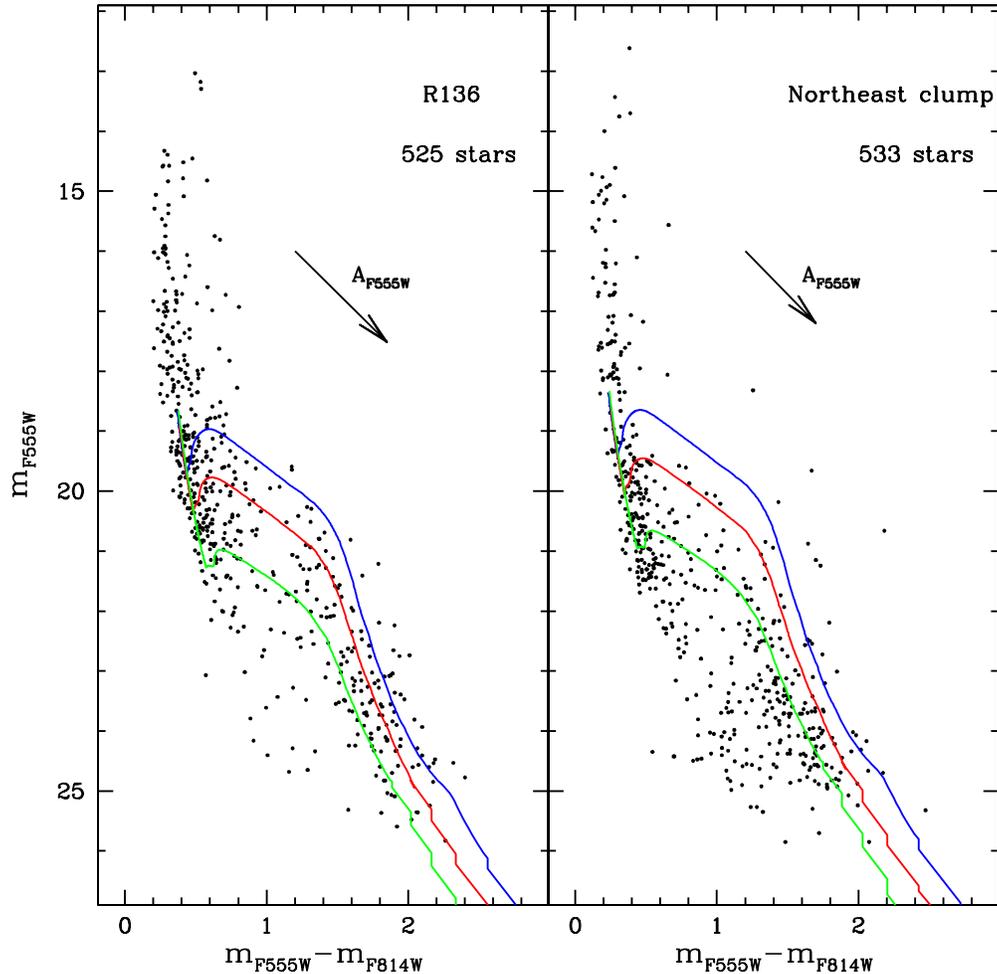
Figure 5. CMDs of m_{F555W} vs. $m_{F555W} - m_{F814W}$ of the stars with photometric error <0.15 mag in both the F555W and F814W filters found within $\sim 10''$ from the center of R136 (left panel) and in a $\sim 14''.4 \times 27''$ box centered on the northeast clump (right panel). Pisa isochrones for PMS stars with metallicity $Z = 0.008$ and an age of 1, 2, and 5 Myr are plotted in blue, red, and green, respectively. In both the CMDs, a distance modulus of 18.5 was assumed. R136 is better reproduced assuming an $A_{F555W} = 1.525$. For the northeast clump $A_{F555W} = 1.207$ is sufficient.

(A color version of this figure is available in the online journal.)

R142 along the ridge of the northeast clump could be associated with R136, but on the other hand, some such objects are also found in older young clusters (e.g., TS3 in NGC 2060; Schild & Testor 1992), possibly as a result of binary evolution. In summary, the information presented here provides strong support for our completely independent recognition of a double system with an age offset between them in the core of 30 Dor.

Characterizing the complex structure of massive star-forming regions such as NGC 2070 is important to understand the early stages of cluster formation. The age difference found between R136 and the northeast clump, as well as their morphology, may indicate that the core of NGC 2070 is the result of a recent or ongoing merger between two sub-clusters. Interestingly from the analysis of the radial velocities of apparently single O stars, V. Hénault-Brunet et al. (2012, submitted) found evidence for an internal rotation in NGC 2070, that can be due to either a recent merger between the main core of NGC 2070 and a secondary cluster or by the agglomeration and clumpiness of the gas.

The majority of the stars studied in V. Hénault-Brunet et al. (2012, submitted) coincides with R136, but five sources coincide with the northeast clump. If the total mass of the system is $\sim 10^5 M_\odot$ (Andersen et al. 2009) then the velocity difference, assuming a distance $d = 4.5$ pc, would be

$v = \sqrt{(2GM/d)} \simeq 13$ Km s^{-1} for a hyperbolic encounter (i.e., 0 energy), and $\simeq 9$ km s^{-1} for a circular orbit. The maximum velocity difference reported by V. Hénault-Brunet et al. (2012, submitted) is ~ 5 km s^{-1}. If R136 and the northeast clump are undergoing a merger, then either we are observing the interaction with a low inclination (which would agree with the fact that we see the tidal tail on the plane of the sky), or the two systems are bound and are falling in with low velocity. A detailed analysis of the mass distribution in the two sub-clusters and a more sophisticated modeling of the two-component interaction will be presented in two forthcoming papers (E. Sabbi et al. 2012, in preparation; M. Gieles et al. 2012, in preparation)

The presence of distinct components in a very young system is also consistent with recent studies of galactic giant molecular clouds (GMCs; Heyer et al. 2009), which contradict the traditional paradigm that GMCs are gravitationally bound systems. Ballesteros-Paredes et al. (2011) suggested that GMCs can undergo a hierarchical gravitational collapse, with the collapse occurring on scales ranging from individual cores to the whole cloud. In this scenario, because of the turbulent fragmentation of a GMC, SF will not be spread over the whole GMC, but will be localized in gravitationally bound pockets of gas (Clark et al. 2005, 2008). Star clusters will be the final products of the

hierarchical merger of such smaller sub-structures (Bonnell et al. 2003; Bate 2009; Federrath et al. 2010).

We finally note that in a recent paper Fujii et al. (2012) suggested that the cuspy density profile of R136 and the large number of massive runaway stars that seem to escape from this cluster are effective signatures of a post-core-collapse star cluster (Mackey & Gilmore 2003). Considering the small age of R136, such an early core collapse would occur only if the cluster had an initial density of $\rho_c \geqslant 10^6\,M_\odot\,\mathrm{pc}^{-3}$, which is considerably higher than the current estimates. Fujii et al. (2012) suggest that an efficient way to speed up the collapse process is to invoke the hierarchical merging of several smaller clusters.

Observational evidence for a hierarchical process of SF comes also from the complex structure of massive star-forming regions such as NGC 604 in M33 (Maíz-Apellániz et al. 2004), or NGC 346 in the Small Magellanic Cloud (Sabbi et al. 2007). Also, Gennaro et al. (2011) suggested that the elongation and mass segregation found in Westerlund 1 may be the footprint of a merger of multiple sub-clusters, formed almost coevally in the parental GMC. If massive star clusters form from mergers of smaller sub-systems, this can also explain the high fraction of rotating globular clusters found in our Galaxy. A study of the radial velocities and/or proper motions of the stars in the two clumps would provide a further test of the merging scenario. Such data set are currently being obtained by us (e.g., V. Hénault-Brunet et al. 2012, submitted; D. J. Lennon et al. 2012, in preparation).

REFERENCES

Andersen, M., Zinnecker, H., Moneti, A., et al. 2009, ApJ, 707, 1347
Anderson, J., Bedin, L. R., Piotto, G., Yadav, R. S., & Bellini, A. 2006, A&A, 454, 1029
Anderson, J., & King, I. R. 2006, PSFs, Photometry and Astrometry for the ACS/WFC (ISR-ACS 2006-01; Baltimore, MD: STScI)
Ballesteros-Paredes, J., Hartmann, L. W., Vázquez-Semadeni, E., Heitsch, F., & Zamora-Avilés, M. A. 2011, MNRAS, 277, 362
Bastian, N., & Goodwin, S. P. 2006, MNRAS, 369, L9
Bate, M. R. 2009, MNRAS, 392, 590
Baume, G., Vázquez, R. A., Carraro, G., & Feinstein, A. 2003, A&A, 402, 549
Belikov, A. N., Hirte, S., Meusinger, H., Piskunov, A. E., & Schilbach, E. 1998, A&A, 332, 575
Bellini, A., Anderson, J., & Bedin, L. R. 2011, PASP, 123, 622
Bellini, A., & Bedin, L. R. 2009, PASP, 121, 1419
Bonnell, I. A., Bate, M. R., & Vine, S. G. 2003, MNRAS, 343, 413
Bosch, G., Terlevich, R., Melnick, J., & Selman, F. 1999, A&AS, 137, 21
Brandl, B. R., Devost, D., Higdon, S.J.U., et al. 2004, ApJS, 154, 188
Campbell, M. A., Evans, C. J., Mackey, A. D., et al. 2010, MNRAS, 405, 421
Cignoni, M., Tosi, M., Sabbi, E., et al. 2010, ApJ, 712, L63
Clark, P. C., Bonnell, I. A., & Klessen, R. S. 2008, MNRAS, 386, 3
Clark, P. C., Bonnell, I. A., Zinnecker, H., & Bate, M. R. 2005, MNRAS, 359, 809
Crowther, P. A., Evans, C. J., Mackey, A. D., et al. 2010, MNRAS, 405, 421
Crowther, P. A., & Walborn, N. R. 2011, MNRAS, 416, 1311
de Koter, A., Heap, S. R., & Hubeny, I. 1998, ApJ, 509, 879
De Marchi, G., Paresce, F., Panagia, N., et al. 2011, ApJ, 739, 27
Elson, R. A., Fall, S. M., & Freeman, K. C. 2987, ApJ, 323, 54
Feast, M. W., Thackeray, A. D., & Wesselink, A. J. 1960, MNRAS, 121, 337
Federrath, C., Banerjee, R., Clark, P. C., & Klessen, R. S. 2010, ApJ, 713, 269
Fujii, M. S., Saitoh, T. R., & Portegies Zwart, S. F. 2012, ApJ, 753, 85
Gennaro, M., Bradner, W., Stolte, A., & Hemmimg, Th. 2011, MNRAS, 412, 2469
Heckman, T. M., Kauffmann, G., Brinchmann, J., et al. 2004, ApJ, 613, 109
Helling, C., Winters, J. M., & Sedlmayr, E. 2000, A&A, 358, 651
Heyer, M., Krawczyk, C., Duval, J., & Jackson, J. M. 2009, ApJ, 699, 1092
Kennicutt, R. C., Jr. 1984, ApJ, 287, 116
Mackey, A. D., & Gilmore, G. F. 2003, MNRAS, 338, 85
Maíz-Apellániz, J., Pérez, E., & Mas-Hesse, J. M. 2004, AJ, 128, 1196
Marigo, P., Girardi, L., Bressan, A., et al. 2008, A&A, 482, 883
Massey, P., & Hunter, D. A. 1998, ApJ, 493, 180
McGregor, P. J., & Hyland, A. R. 1981, ApJ, 250, 116
Melnick, J. 1985, A&A, 153, 235
Meurer, G. R., Heckman, T. M., Lehner, M. D., Leitherer, C., & Lowenthal, J. 1997, AJ, 114, 54
Meylan, G. 1993, in ASP Conf. Ser. 48, The Globular Cluster-Galaxy Connection, ed. G. H. Smit & J. P. Brodie (San Francisco, CA: ASP), 588
Moffat, A. F. J., Niemela, V. S., Phillips, M. M., Chu, Y.-H., & Seggewiss, W. 1987, ApJ, 312, 612
Nikolaev, S., Drake, A. J., Keller, S. C., et al. 2004, ApJ, 601, 260
Parker, J. W. 1993, AJ, 106, 560
Sabbi, E., Sirianni, M., Nota, A., et al. 2007, AJ, 133, 2430
Schaefer, G. H., Simon, M., Prato, L., & Barman, T. 2008, AJ, 135, 1659
Schild, H., & Testor, G. 1992, A&AS, 92, 729
Selman, F., Melnick, J., Bosch, G., & Terlevich, R. 1999, A&A, 347, 532
Shapley, A. E., Steidel, C. C., Pettini, M., & Adelberger, K. L. 2003, ApJ, 588, 65
Stauffer, J. R. 1980, AJ, 85, 1341
Tognelli, E., Prada Moroni, P. G., & Degl'Innocenti, S. 2011, A&A, 533A, 109
Walborn, N. R., & Blades, J. C. 1997, ApJS, 112, 457